

Validation of Direct Green's Function Seismograms

Fred Pollitz¹

¹ U.S. Geological Survey, Menlo Park, CA 94025, USA

February 25, 2011

Here we compare Direct Green's Function seismograms on a spherically symmetric reference model with the corresponding analytic solutions on a homogeneous full space. The reference model is a homogeneous sphere of radius 300 km with $\kappa_0 = 50$ GPa, $\mu_0 = 30$ GPa, and $\rho_0 = 3000$ kg m⁻³. We synthesize the seismic wavefield using 512 complex-valued frequencies ω' just below the real axis ($\omega' = \omega - i\gamma$) with a maximum real-part of $2\pi/\Delta t$ Hz ($\Delta t = 0.07$ sec) and a maximum spherical harmonic degree of 3000. The source and observation-point depths are 19 km and 29 km, respectively.

A Cartesian coordinate system is erected such that the z -axis passes through the pole of the spherical model. A point source with a step function time dependence is placed at 20 km depth on the z -axis, and a receiver is placed at offset r from the z -axis as measured from the source. For the Direct Green's Function, the velocity of a given component is given by the time derivative of eqn 37 of Friederich and Dalkolmo (1995) with an acausal frequency filter consisting of a cosine taper between the corner frequency and twice the corner frequency. For an isotropic source with the diagonal elements of the moment tensor equal to $M(t) = M_0 H(t)$, the analytic solution for vector displacement in a homogeneous full space is the Stokes solution given by eqn (4.29) of Aki and Richards (1980), which in the frequency domain takes the form

$$\tilde{\mathbf{u}}^0(\mathbf{r}; \omega') = \frac{1}{4\pi\rho v_p^2 r^2} \left[1 + i\frac{\omega' r}{v_p} \right] \exp\left(-i\frac{\omega' r}{v_p}\right) \frac{M_0}{i\omega'} \hat{\mathbf{r}} \quad (1)$$

where $v_p = \sqrt{(\kappa + (4/3)\mu)/\rho}$ and $\omega' = \omega - i\gamma$. For a shear dislocation on a vertical plane, the non-zero moment tensor components are $M_{xy} = M_{yx} = M_0 H(t)$, where x and y are horizontal coordinates. For a receiver offset from the source a distance r in the x -direction, the analytic solution for the transverse-component displacement in the frequency domain is again derived from eqn (4.29) of Aki and Richards (1980):

$$\begin{aligned} \tilde{\mathbf{u}}^0(\mathbf{r}; \omega') = & \left\{ \frac{i\omega'}{4\pi\rho v_s^3 r} \exp\left(-i\frac{\omega' r}{v_s}\right) - \frac{3}{2\pi\rho\omega'^2 r^4} \left[\left(1 + \frac{i\omega' r}{v_s} - \frac{1}{2} \left(\frac{\omega' r}{v_s} \right)^2 \right) \exp\left(-i\frac{\omega' r}{v_s}\right) \right. \right. \\ & \left. \left. - \left(1 + \frac{i\omega' r}{v_p} - \frac{1}{3} \left(\frac{\omega' r}{v_p} \right)^2 \right) \exp\left(-i\frac{\omega' r}{v_p}\right) \right] \right\} \frac{M_0}{i\omega'} \hat{\mathbf{y}} \end{aligned} \quad (2)$$

where $v_s = \sqrt{\mu/\rho}$. Attenuation in the homogeneous full space is simulated by perturbing seismic wave velocities by an amount proportional to the bulk and shear anelasticities Q_κ^{-1} and Q_β^{-1} , e.g. eqns (9.57)-(9.60) of Dahlen and Tromp (1998).

For an isotropic source, Figures 1a show a comparison between the Direct Green's Function and analytic velocity at source-receiver distances from 10 to 40 km using $Q_\beta = 25$ and $Q_\kappa = 2.5 \times Q_\beta$ at a reference frequency of 1 Hz. The good agreement indicates that the Direct Green's Function accurately simulates P-wave propagation and attenuation. Small-amplitude arrivals long after the P-wave pulse are reflections off the free surface.

Figures 1b shows a comparison between the Direct Green's Function and analytic solution for transverse-component velocity using $Q_\beta = 25$. These comparisons indicate that S-wave propagation and attenuation are well replicated by the Direct Green's Function. The first term in eqn 2 represents the S-wave pulse, which dominates in the far field. Eqn 2 predicts that in the near field, a small amount of energy arrives at the P-wave velocity ahead of the S-wave pulse, and this feature is also replicated in the mode sum. Figure 2 shows the same comparison with $Q_\beta = Q_\kappa = \infty$

In these examples, the source-receiver incidence angle varies from 0 (for offsets of 10 km) to 76° (for offsets of 40 km), showing that the Direct Green's Function method is handling both vertical and horizontal wave propagation.

References

- Aki, K. and Richards, P. G. (1980). *Quantitative Seismology*, volume 1. W.H. Freeman and Company, San Francisco.
- Dahlen, F. A. and Tromp, J. (1998). *Theoretical Global Seismology*. Princeton University Press, Princeton, N.J.
- Friederich, W. and Dalkolmo, J. (1995). Complete synthetic seismograms for a spherically symmetric earth by a numerical computation of the greens function in the frequency domain. *Geophys. J. Int.*, 122:537–550.

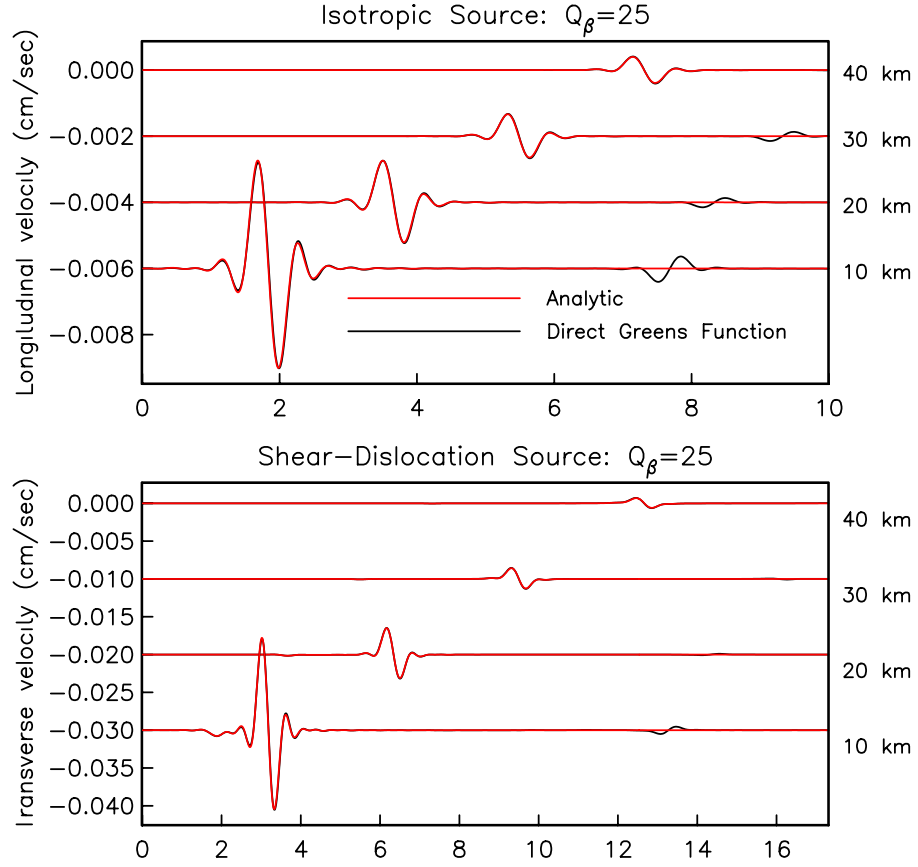


Figure 1: Comparison between Direct Green's Function and analytic velocity seismograms obtained for the indicated source types and source-receiver offsets (section 2.5). A corner frequency $\omega_r = 2\pi \times 1.43$ rad/sec is used. (a) Isotropic source, $Q_\beta = 25$, $Q_\kappa = 2.5 \times Q_\beta$. (b) Shear dislocation, $Q_\beta = 25$.

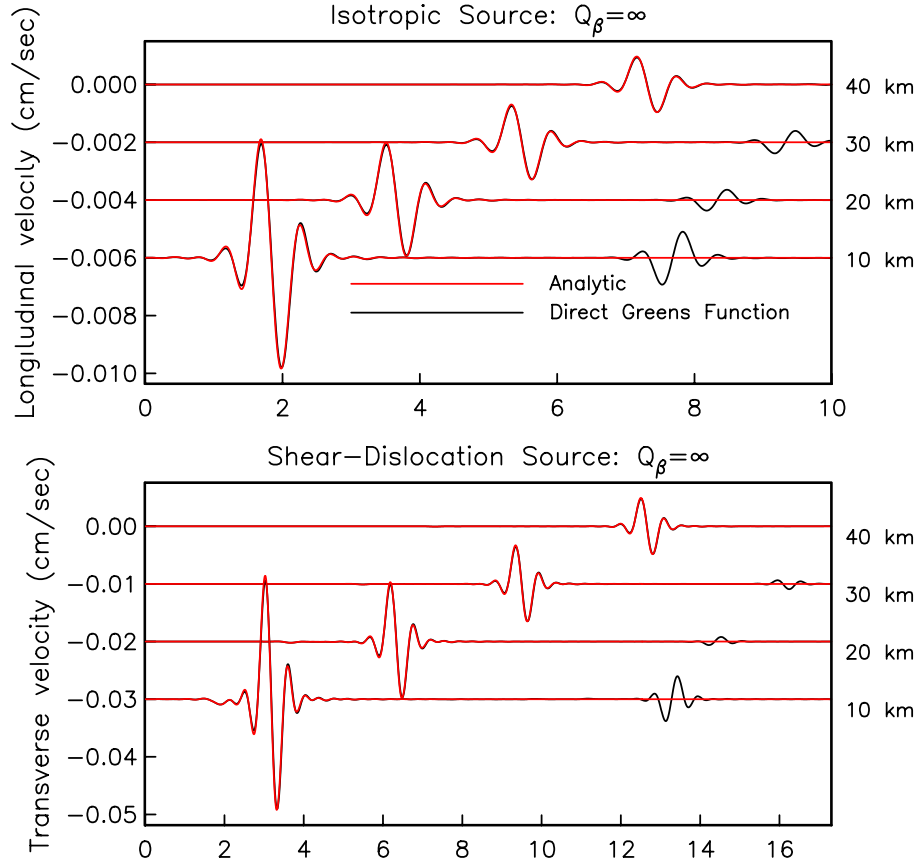


Figure 2: Comparison between Direct Green's Function and analytic velocity seismograms obtained for the indicated source types and source-receiver offsets (section 2.5). A corner frequency $\omega_r = 2\pi \times 1.43$ rad/sec is used. (a) Isotropic source, $Q_\beta = \infty$, $Q_\kappa = \infty$. (b) Shear dislocation, $Q_\beta = \infty$.